Journal of Fluorescence, Vol. 8, No. 4, 1998

Fluorescence Decay of Natural Organic Matter (NOM)—Influence of Fractionation, Oxidation, and Metal Ion Complexation

M. U. Kumke,[1] C. Tiseanu,[1] G. Abbt-Braun,[1] and F. H. Frimmel[1,2]

Received January 25, 1998; accepted August 12, 1998

Time-resolved fluorescence measurements of aquatic natural organic matter (NOM) derived from different origins were performed using the time-correlated single-photon counting technique. The obtained experimental data were analyzed with nonlinear least-squares (NLLS) algorithms. The results of a global analysis with three exponential decay terms were compared with the results obtained in a distribution analysis (exponential series method; ESM). Fulvic acid fractions from a bog lake water, from a brown coal production effluent, and from a soil seepage water as well as NOM from a municipal waste water were investigated. The influence of the emission wavelength on the NOM fluorescence decay was monitored. Furthermore, the influence of fractionation using size exclusion chromatography, of ozonation, and of metal ion complexation on the fluorescence decay of the NOM samples was investigated.

KEY WORDS: Natural organic matter; humic substances; time-resolved fluorescence; distribution analysis.

INTRODUCTION

In the aquatic environment the transport and transformation of organic and inorganic contaminants are closely related to the presence of natural organic matter (NOM). Therefore, the characterization of NOM and of its interaction processes with xenobiotics is indispensable.

Recently, efforts were concentrated in investigating NOM using time-independent techniques and neglecting the influence of molecular motions of NOM molecules. These *steady-state* methods yielded information on molecular weight distributions [1,2] and the content of structural components such as phenolic and carboxylic groups [3–6], and even some basic structures inside the NOM matrix responsible for light absorption and fluorescence were concluded [3,4,7]. Fluorescence spectroscopic techniques are powerful tools for the investigation of molecular processes and structures. During the last decades steady-state fluorescence techniques have been applied successfully in NOM research [8–12]. Especially, the synchronous fluorescence spectroscopy has proven to yield valuable results in the characterization of NOM [10,12–14]. Recently, the application of time-resolved fluorescence techniques was introduced into NOM research [15–20]. For all NOM samples investigated in time-resolved fluorescence measurements, a highly complex fluorescence decay has been reported [17–21]. Different approaches to data analysis have been applied: (a) a robust approach that selects the point of time the initial fluorescence intensity has decayed to $1/e$ (or $1/3e$) to characterize the fluorescence decay [22,23], (b) the use of a small number of exponential decay functions assuming a low number of fluorescence components (discrete component approach; DCA) [17,20,21], and (c) the assumption of a large number of decay functions ($i \approx 100$) resulting in a distribution of decay times [19,21]. The robust approach will not add substantial

[1] Water Chemistry Division, Engler-Bunte-Institute, University of Karlsruhe, Richard-Willstätter-Allee 5, 76131 Karlsruhe, Germany.
[2] To whom correspondence should be addressed.

1053-0509/98/1200-0309$15.00/0

information in the understanding of the NOM fluorescence decay, although it offers a simple way to obtain an additional characterization parameter for NOM [22,23]. Using the DCA at least three exponential decay terms were necessary for a satisfying data representation of the NOM fluorescence decay (judged on the χ^2 value and the randomness of the residuals) [17,20,21]. However, the interpretation of the parameters found is crucial because they were operationally defined and should not be mistaken for real fluorophores without further structural information of NOM. In the application of decay time distributions no preassumed number of fluorescence decay components is introduced. McGown *et al.* used the maximum entropy method (MEM) and found a trimodal distribution of decay times for different NOM samples [19]. Kumke *et al.* applied the exponential series method (ESM) in the analysis of NOM samples of different aquatic origin and found multimodal decay time distributions [21].

The high complexity of the NOM fluorescence decay could be caused by several intra- and intermolecular processes and structural features of the NOM matrix such as a large number of different fluorophores or a small number of fluorophores in many molecular environments. Possible intra- and intermolecular interactions are energy transfer between fluorophores and reorientation processes (e.g., proton transfer reactions).

The objective of the presented work was to investigate the fluorescence decay of natural organic matter (NOM) of different origins. By monitoring the influence of oxidation, of fractionation, and of metal ion complexation on the time-resolved fluorescence of NOM, the relationship between observed fluorescence and structure was further probed.

EXPERIMENTAL

Time-Resolved Fluorescence Measurements

Time-resolved fluorescence measurements were performed using a FL900CDT fluorescence spectrometer (Edinburgh Analytical Instruments, Research Park, Riccarton, Currie, Edinburgh UK) in the time-correlated single-photon counting mode. The instrument was set up in a T-geometry format with two analyzing detection channels. The focal length of the monochromators in the excitation and emission channels was 300 mm, with an aperture of f/4.2 (optical configuration: symmetrical Czerny–Turner). The grating of the excitation monochromator was blazed at 250 nm and the gratings of the emission monochromators were blazed at 500 nm for optimal performance. The linear dispersion of the monochromators was 1.8 nm/mm, which, together with the slit width, determines the spectral bandpass of the fluorescence measurements. For the detection a photomultiplier tube (PMT) R1527 (Hamamatsu) with a rise time of 2.2 ns was used. A nF900 nanosecond flash lamp (Edinburgh Analytical Instruments) filled with nitrogen gas (1 bar, 6.6 kV, 0.3-mm electrode separation, operated at 40 kHz) was used for the excitation of the samples. A multichannel analyzer (MCA) Norland 5000 (Viking Instruments Inc., 128 Owen Road, Madison, WI) was operated in the pulse height analysis mode. The memory of the MCA Norland 5000 consists of 4096 channels. In the typical T-geometry format experiment 1024 channels of the MCA were attributed to each detection channel.

For data analysis the commercial software of Edinburgh Instruments was used. In addition to the standard software features (multiexponential data fitting), level 2 software was chosen for the decay time distribution analysis and the global analysis.

In order to get reliable results in an acceptable period of time the experiments were performed at a count level of 5×10^4 cpm. The measurement time was usually below 4 h and the stability of the time profile of the excitation pulse was controlled by monitoring the fluorescence decay of the NOM samples and the excitation pulse in cycles of 5000 cpm per cycle.

The excitation wavelength in the time-resolved fluorescence experiments was 314 nm. The experiments were typically run at a time base of 100 ns, with 5 ns delay of the stop PMT. The NOM fluorescence was investigated between λ_{em} = 390 nm and λ_{em} = 590 nm. In the time-resolved fluorescence experiments the emission bandpass was 9 nm in both detection channels.

In general, the counting rate was less than 1% for the NOM samples under investigation, and therefore, pile-up problems in the decay time data analysis were not likely to occur. The experimental data were analyzed with nonlinear least-squares (NLLS) algorithms based on the method of Marquardt. The results of the data-fitting procedures were judged by the χ^2 value and the randomness of the weighted residuals. In the data fitting, only the fluorescence decay was taken into account. Therefore, it was not necessary to introduce a shift term into the data analysis.

Samples and Sample Treatment

In the fluorescence experiments a dissolved organic carbon (DOC) concentration of 5. . .10 mg/L was used. Unless noted otherwise the samples were dissolved in

Table I. Basic Parameters of the Aquatic NOM Samples [$Q = (a_{254\ nm}/a_{436\ nm})$], Where a Is the Specific Absorption Coefficient at Wavelength λ

	H/C	O/C	N/C	S/C	Q (pH 7)
Bog lake water FA	0.83	0.57	0.01	0.005	12.6
Municipal wastewater effluent	1.19	0.49	0.05	0.02	1.8
Effluent from brown coal production (FA)	1.04	0.50	0.03	0.07	9.8
Soil seepage water FA	0.82	0.59	0.01	0.002	13

deionized water (MilliQ water purification system) at a pH value of 6. . .7.

The NOM samples were of different aquatic origin, with the exception of the soil seepage water. Table I summarizes the samples investigated. The isolation procedure was based on the XAD method of Mantoura and Riley using XAD-8 resins and was described by Abbt-Braun *et al.* [24].

Fractionation

The FA isolated of a bog lake water and of a soil seepage water were further fractionated by size exclusion gel chromatography (TSK HW40S, Merck). The process was operationally defined by collecting fractions of the eluting NOM sample at preset times. The soil seepage water FA was divided into four and the bog lake water FA into three fractions, respectively. To obtain a sufficient amount of each fraction the procedure was repeated several times. The fluorescence results shown represent the average of the runs of fractionation. In the time-resolved fluorescence measurements an excitation wavelength λ_{ex} = 314 nm and an emission wavelength λ_{em} = 450 nm were used.

Ozonation

The ozonation of the NOM sample was performed in a vessel (height, 0.35 m; diameter, 0.065 m) stirred by a magnetic stirrer. For the dispersion of the ozone the reactor was equipped with a porous glass frit. The ozone concentration in the gaseous phase was measured before and after passing the reactor using two UV detectors at a detection wavelength of 254 nm [25]. The bog lake water (DOC = 15 mg/L) was filtered (0.45 μm) and ozonated for a maximum of 20 min. During this ozonation samples were taken at preset times.

DATA EVALUATION

Data Analysis Using a Small Set of Exponential Functions with Linked Decay Times (Global Analysis)

The experimental data were evaluated with a sum of three exponential terms [eq. (1)]:

$$I(t) = \sum_{i=1}^{3} B_i \cdot e - \frac{t}{\tau_i} \qquad (1)$$

Here, $I(t)$ is the fluorescence intensity of the sample dependent on time t after the excitation pulse, τ_i is the fluorescence decay time, and B_i is the related fractional intensity. The relative fractional intensity A_i of each component of the total fluorescence decay is given by Eq. (2):

$$A_i = \frac{B_i\tau_i}{B_1\tau_1 + B_2\tau_2 + B_3\tau_3} \quad \text{with} \quad i = 1,2,3 \qquad (2)$$

In the global analysis the three decay times were linked during the fitting process of a set of experimental data (e.g., for different emission wavelengths or different times of ozonation) to find the set of fluorescence decay times optimized for all decay data sets introduced, and only the fractional intensities were fitted independently for each decay data set.

Exponential Series Method (ESM)

In the ESM approach no initial model for the fluorescence decay was introduced into the data analysis. Using the exponential series method (ESM) no assumption was initially made about the number of fluorophores responsible for the fluorescence decay rather than starting with a flat distribution of exponential decays evenly spaced on a logarithmic scale [26–29]. The number of exponential terms could be up to 100 distributed over several decades of nanoseconds. The fractional intensities A_i of each decay time were varied during the fitting procedure. To avoid bias and to vary the decay times, the fitting was performed with different numbers of decay time and different time intervals in terms of lower and upper limits of the flat starting distribution of fluorescence decay times. For artificial decay time components introduced due to noise in the experimental data, it is expected that these components are influenced by the different start conditions for the fit. Real decay time components should be independent of the start parameters.

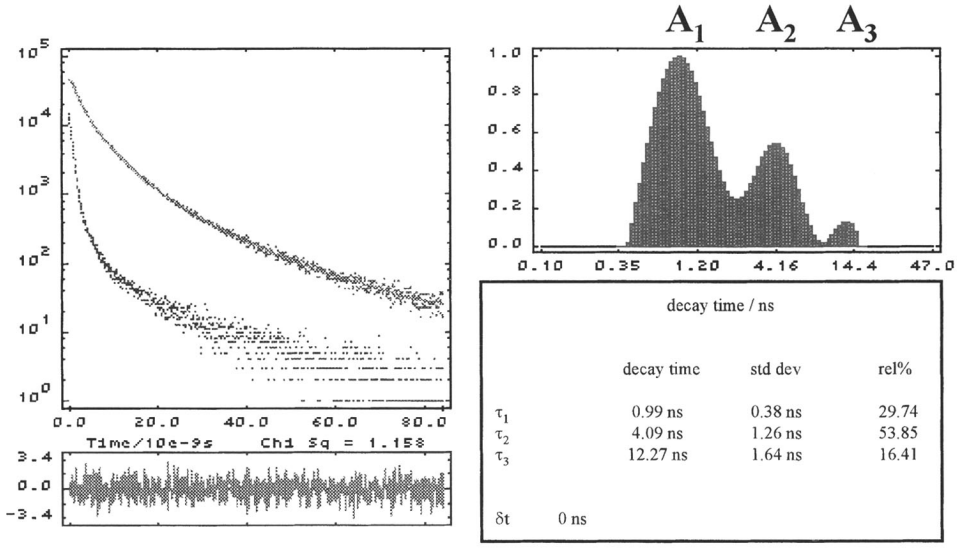

Fig. 1. ESM analysis of NOM derived of a municipal waste water. The experimental data, the fitted curve, and the corresponding residuals are shown at the left. Right: The obtained distribution of fluorescence decay times and the calculated mean decay times and related fractional intensities. For the fit 100 decay terms in a time range between 0.1 and 50 ns were used (λ_{ex} = 314 nm, λ_{em} = 420 nm, DOC = 10 mg/L, pH 6.5).

In general, for the data evaluation a number of 100 fluorescence decay times was chosen, with the lower limit at 0.1 ns and the upper limit at 50 ns.

RESULTS AND DISCUSSION

For all NOM samples investigated the observed fluorescence decay was highly complex. The experimental NOM fluorescence data were fitted in terms of a mathematical description by a sum of three exponential decay terms (DCA) and by a distribution of a large number of exponential decay terms (ESM). The fluorescence decay distribution analysis worked without a preassumed number of fluorescing components; only the time range was preset in the data analysis and should therefore be less biased.

In the data analysis a parameter set of fluorescence decay times τ_x and related fractional intensities A_x was obtained. These parameter sets were *operationally defined*. It should be stressed that their interpretation in terms of real physical fluorophores (or groups of fluorophores in case of the distribution analysis) has to be done very carefully.

Fluorescence Decay of NOM Samples of Different Aquatic Origins—Influence of the Emission Wavelength

In order to overcome the lack of reliable literature data on time-resolved fluorescence, measurements of NOM of different aquatic origin were performed. The obtained data were evaluated with three exponential decay terms (DCA; global analysis) as well as with a distribution of fluorescence decay times (ESM). The elemental composition and the spectral absorption of the NOM samples investigated are summarized in Table I.

Figure 1 shows data on the fluorescence decay of a municipal waste water and results of the distribution analysis. For all NOM samples investigated the distribution analysis yielded a trimodal distribution. The results presented are in good agreement with previously reported data [17,19,20]. McGown *et al.* applied a different distribution analysis (maximum entropy method; MEM) and found a trimodal distribution for the investigated humic substance as well.

The fluorescence decays of the NOM samples (a municipal wastewater effluent, a bog lake water FA, and a brown coal production effluent FA) were monitored in the emission wavelength range between λ_{em} = 390 nm and λ_{em} = 550 nm. For all fluorescence emission wavelengths the ESM analysis recovered a trimodal distribution and variations of the calculated mean fluorescence decay times of each peak were smaller than 10% for each NOM sample. It is interesting to note that the mean fluorescence decay times of the three NOM samples were quite similar (see Table II).

The mean fluorescence decay times reported by McGown *et al.* were found to be in the same time range ($\tau_1 < 1$ ns, $\tau_2 \sim 3$ ns, $\tau_3 \sim 10$ ns) using MEM analysis

Table II. Average Mean Fluorescence Decay Times of the Three NOM Samples Investigated in the Emission Wavelength Range Between λ_{em} = 390 and λ_{em} = 530 nm

	Global analysis (ns)			Distribution analysis (ns)		
Sample	τ_1	τ_2	τ_3	τ_1	τ_2	τ_3
Bog lake water FA	1.1 ± 0.1	4.1 ± 0.3	11.8 ± 0.9	1 ± 0.1	4.3 ± 0.3	14.6 ± 1.2
Municipal wastewater effluent	1.1 ± 0.2	4.4 ± 0.4	12.6 ± 1	1 ± 0.2	4.1 ± 0.2	12.8 ± 0.9
Effluent from brown coal production (FA)	1.2 ± 0.1	4.3 ± 0.2	12.4 ± 1.1	1.1 ± 0.2	4.1 ± 0.5	14.8 ± 2.7

[19]. Langford and Cook investigated NOM samples derived from soil organic matter. They applied a DCA with three-exponential decay functions in the data analysis. They reported decay times shorter compared to the decay times presented here and found by McGown *et al.*, probably due to the fact that the samples were of soil origin [20].

In contrast to the fluorescence decay times, the relative fractional intensities were found to be strongly dependent on the fluorescence emission wavelength for each of the NOM samples investigated in this study. Figure 2 shows the relative fractional intensities calculated in the distribution analysis for the three mean fluorescence decay times. These results are in good agreement with previously reported measurements of FA of different aquatic origins [21].

For further discussion the shortest decay time component is referred to as τ_1 and the related relative fractional intensity as A_1(τ_2, A_2 and τ_3, A_3, respectively). For τ_1 = 1.1 ns the relative fractional intensity decreased for all investigated NOM samples with increasing emission wavelength; for the FA of a brown coal production effluent it started to rise again for emission wavelengths above 440 nm. Overall, for this NOM sample the relative fractional intensity of τ_1 decreased from 47% at 390 nm to about 23% at 510 nm. At the same time its decay time τ_2 = 4.1 ns increased in its fractional intensity from 40% at 390 nm to almost 67% at 510 nm. The relative fractional intensity of the third fluorescence decay time (τ_3 = 14.8 ns) was almost unchanged over the whole investigated emission wavelength range. The bog lake water FA showed a comparable trend in the first fluorescence decay time, τ_1 = 1 ns. Its fractional intensity A_1 decreased but to a lesser extent. The fractional intensities of τ_2 as well as τ_3 changed with the fluorescence emission wavelength. Finally, the NOM of a municipal wastewater effluent showed a steady decrease in the fractional intensity of τ_1, no change for the fractional intensity of τ_2, and a steady increase for the fractional intensity of the third fluorescence decay time. Because

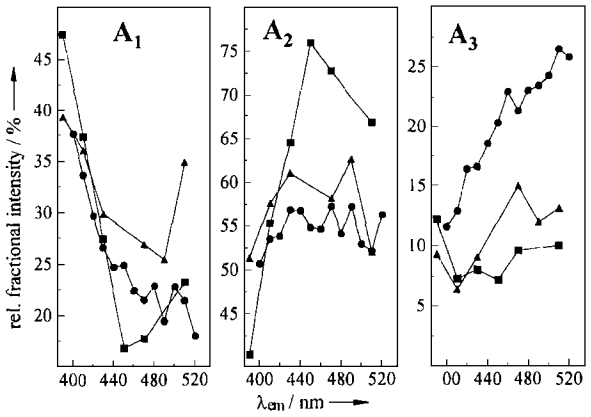

Fig. 2. Calculated relative fractional intensities of the three mean fluorescence decay times in the emission wavelength range investigated. The results for a bog lake water FA (triangle), a brown coal production effluent FA (squares), and a municipal wastewater effluent (circles) (λ_{ex} = 314 nm, DOC = 10 mg/L, pH 6.5) are shown.

the municipal waste water is relatively young in terms of genesis, its content of fulvic acid-like matter is high and therefore determined the observed fluorescence.

The experimental data were also evaluated using three exponential decay functions with the three fluorescence decay times linked in the fitting process (global analysis). For all three NOM samples investigated a global χ^2 value better than 1.2 was obtained in the data analysis. It is interesting to note that the results of the global analysis yielded the same trends in the emission wavelength dependence of the fractional intensities that were found in the distribution analysis. In Table II the calculated fluorescence decay times are compared with the results obtained in the distribution analysis. It can be seen that both data evaluation methods yielded the similar fluorescence decay times.

The elemental composition of the three samples was highly different regarding the content of heteroatoms (especially of sulfur and nitrogen; see Table I). The three investigated NOM samples had a relative content

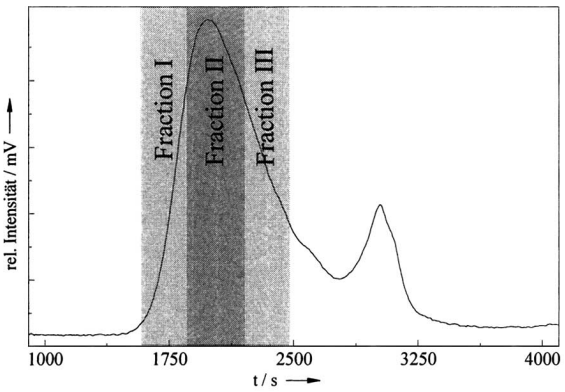

Fig. 3. Size exclusion chromatogram (SEC) of a bog lake water FA used in the fractionation experiments (TSK gel, DOC detection). Shown schematically are the operationally defined cutoff times for the fractionation.

of sulfur in the order of brown coal production effluent FA > municipal wastewater effluent > bog lake water FA. But in the case of the relative nitrogen content the order has to be changed to municipal wastewater effluent > brown coal production effluent FA > bog lake water FA. It is interesting to compare the observed differences in the fractional contributions A_1, A_2, and A_3 for the three NOM samples with their different heteroatom contents. For all NOM samples the trend of A_1 was quite similar, but the FA of the effluent of brown coal industry (highest sulfur content) showed the strongest dependence on the emission wavelength for A_2, and for the municipal wastewater effluent (highest nitrogen content) the most pronounced influence on A_3 was observed (refer to Table I and Fig. 2, respectively).

Fractionation of NOM

Figure 3 shows a size exclusion chromatogram of the bog lake water FA. Schematically shown are the cutoff times in the fractionation of the NOM sample. The time-resolved fluorescence measurements of the fractions revealed only a small difference in the fluorescence decay. The calculated fluorescence decay time pattern in the distribution analysis as well as the global analysis of the experimental data showed minor differences between each fraction. For the bog lake water FA the data analysis of the three fractions I, II, and III and the original FA yielded, within the error of the measurements, identical decay times and fractional intensities. The decay time distribution pattern showed a small change in the decay time regime between 2 and 15 ns, with an increase going from fraction I, with a higher mean nominal molar mass, to fraction III, with a lower mean nominal molar mass. These results were in agreement with data obtained for other properties of the NOM fractions I. . .III of the bog lake water (e.g., UV/vis, proton capacities), where only very small differences were detectable between the fractions.

For the soil seepage water FA and its fractions I. . .IV (see Table III), the differences were more pronounced. With increasing mean nominal molar mass, the contribution of the longer fluorescence decay times relative to the 1-ns peak was amplified (see Table III and Fig. 4). Judged by the fluorescence decay time distribution, fractions III and IV were most closely related to the original soil seepage water FA.

The two fractions with a nominal molar mass smaller than the original FA seemed to determine the fluorescence decay. For these two fractions the calculated fluorescence decay time pattern in the distribution analysis as well as the results of a global analysis was similar to the original FA. Fractions I and II showed a clear decrease in the contribution of longer decay times (see Fig. 4). Considering the relative contributions of each fraction to the total dissolved organic carbon of the original sample, fractions III and IV represent approx. 80% which has to be taken into account in the interpretation of the data (see Table III).

Ozonation of Bog Lake Water

In a previous paper the results of ozonation of NOM samples of different origins were reported [21]. In the distribution analysis it was found that due to the ozonation, the relative contributions of fluorescence decay times in the time range below 1.5 ns (''fast-decaying components'') and above 1.5 ns (''slow-decaying components'') were changed. The contribution of decay times shorter than 1.5 ns appeared to be increased relative to the longer fluorescence decay times. This was interpreted in terms of a decrease in the molar mass supported by the results of gel chromatography.

For further investigation we performed experiments with bog lake water under different times of exposure to O_3. The measurement of the dissolved organic carbon (DOC) concentration revealed no significant change during the ozonation ($\approx$15 mg/L). In steady-state fluorescence experiments the fluorescence intensity was increased within the first 5 min of ozonation and decreased with further ozonation, with only a slight spectral change. The initial increase in fluorescence intensity could be due to a decrease in the color of the sample solution, which would have resulted in a reduction of the ''inner-filter'' effect. The absorption of the bog lake

Table III. Fractionation of a Soil Seepage Water FA Using SEC (TSK Gel)[a]

Sample	Mean nominal molar mass (g/mol)	Relative portion of DOC (%)	A_1 (%) (τ_1 = 1 ± 0.1 ns)	A_2 (%) (τ_2 = 3.9 ± 0.4 ns)	A_3 (%) (τ_3 = 10.6 ± 0.7 ns)
Soil seepage water FA	857	100	22.8	46.4	30.8
Fraction I	969	6	39.8	42.1	18.04
Fraction II	850	11	33.3	42	24.7
Fraction III	716	45	23.3	48.5	28.2
Fraction IV	654	35	20.6	50.7	28.7

[a] The mean nominal molar mass was determined relative to a standard (polyethylenglycol oxide; PEO). In the time-resolved fluorescence measurements an excitation wavelength λ_{ex} = 314 nm was used in combination with a detection wavelength of 450 nm. In the measurements the spectral bandpass was set to 9 nm.

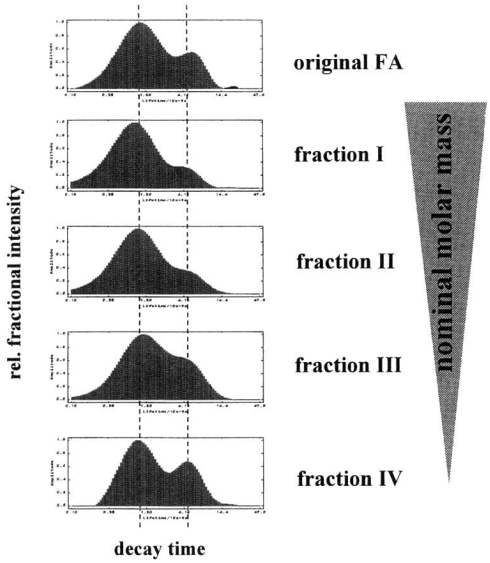

Fig. 4. Distribution analysis of a soil seepage water FA and its fractions I, II, III, and IV, with mean nominal molar masses of 857, 969, 850, 716, and 654 g/mol, respectively (λ_{ex} = 314 nm, λ_{em} = 450 nm, DOC = 10 mg/L, pH 5; PEO standard for the determination of the nominal masses in the SEC).

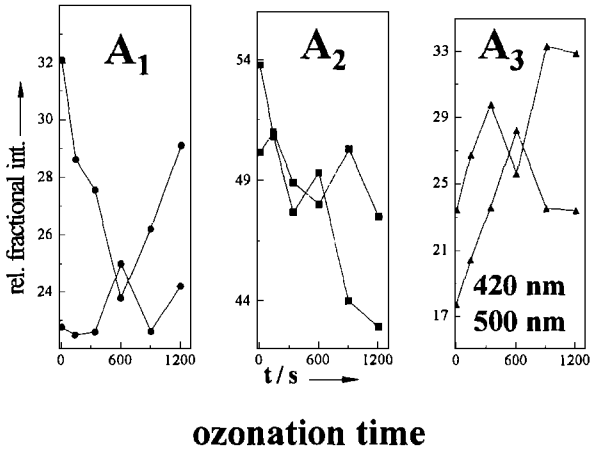

Fig. 5a. Ozonation of a bog lake water (DOC = 15 mg/L, pH 6, λ_{ex} = 314 nm) monitored at two emission wavelengths (λ_{em1} = 420 nm and λ_{em2} = 500 nm). The fractional intensities calculated in the global analysis approach with three linked fluorescence decay times (τ_1 = 0.8 ± 0.1 ns, τ_2 = 3.4 ± 0.3 ns, and τ_3 = 9.7 ± 0.7 ns) at different times of ozone treatment are shown.

water decreased from 0.06 before ozonation down to 0.02 after 20 min of ozone treatment. The absorbed ozone concentration of the reaction solution was approximately 10 mg/L at t = 20 min.

Time-resolved fluorescence measurements were performed at two emission wavelengths (420 and 500 nm). In the distribution analysis the recently described trend of a relative decrease in the longer fluorescence decay times in favor of the shorter time domain was confirmed [21]. During the time course of the ozonation this tendency became more pronounced. Furthermore, a dependence of the observed trend on the detection wavelength in the time-resolved fluorescence measurements was found. In Fig. 5a the results for the global analysis approach with three linked fluorescence decay times are presented. Shown are the fractional intensities of the three fluorescence decay times (τ_1 = 0.8 ± 0.1 ns, τ_2 = 3.4 ± 0.3 ns, and τ_3 = 9.7 ± 0.7 ns, respectively) in the course of the ozonation process.

In the distribution analysis the obtained fluorescence decay time pattern was changed due to the ozonation and the quite resolved three main fluorescence decay time maxima were lost, which went along with the observed changes of the gel chromatographic separation, in which the higher molar mass fraction was reduced and the contribution of organic compounds with a low molar mass (see Fig. 5b; "salt boundary") was increased. The observed changes in the fluorescence decay due to ozonation were dependent on the emission wavelength. The fractional intensities A_1, A_2, and A_3 showed a different influence of the ozonation process.

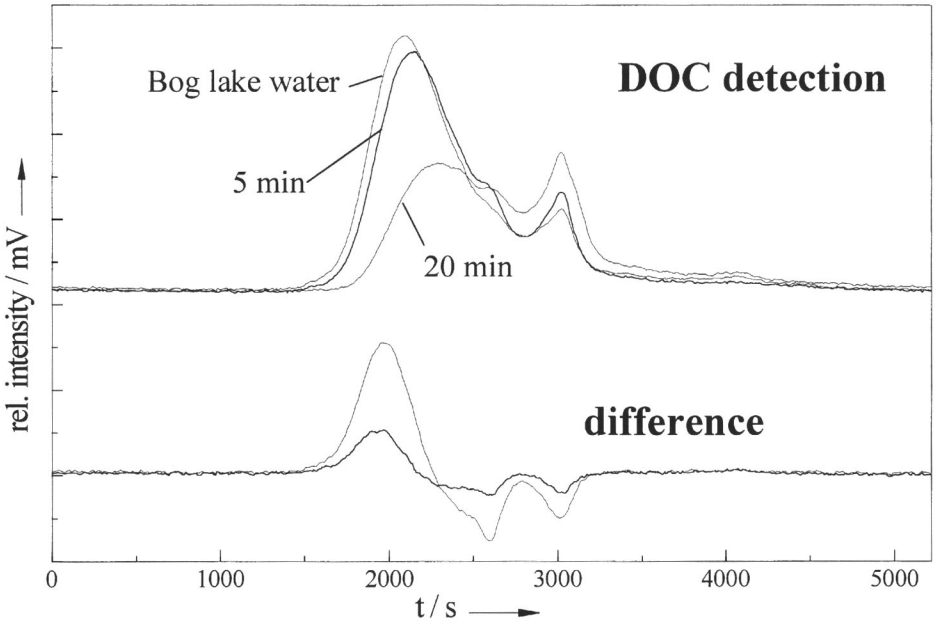

Fig. 5b. SEC of a bog lake water before and after ozonation (5- and 20-min ozone treatment).

A comparison on a relative base of the emission wavelength dependence for the influence of the ozonation process was made. In Fig. 5a the emission wavelength dependence of the ozonation for the calculated fractional intensities in the global analysis is summarized. Considering that different fluorescent structures were attacked to a different extent by the ozone, the observed dependence of the change in the fluorescence decay at the two emission wavelengths can be understood.

Effects of Metal Ion Complexation on the Observed Fluorescence Decay of NOM

For the fluorescence intensity of NOM, quenching was observed upon metal ion binding. The degree of fluorescence quenching was dependent on the metal ion. For copper and iron high fluorescence quenching efficiencies were reported, whereas manganese, lead, and cadmium were rather weak fluorescence quenchers [30,31]. Often the observed quenching of the NOM fluorescence intensity is used to determine binding constants for the metal ions. The mechanism of the fluorescence quenching process is only poorly understood. Neither has the reason for the different quenching efficiencies of different metal ions been fully investigated, nor is the connection between NOM binding sites and fluorophores clear. The application of time-resolved fluorescence methods is suitable to investigate the dynamic interaction processes between metal ions and NOM. Bidoglio *et al.* investigated the luminescence decay of terbium and europium in the presence of NOM, but because of the NOM fluorescence, no conclusions were made about an interaction mechanism [32].

Our preliminary results revealed no effects of copper on the fluorescence decay of a bog lake water FA, although the fluorescence intensity was strongly quenched. Experiments were performed for different emission wavelengths in the range between 400 and 550 nm as well as for two different excitation wavelengths (314 and 357 nm, respectively) at pH 5 with a DOC concentration of 10 mg/L. In the experiments no bulk precipitation was apparent. The formation of small particulates (e.g., colloids) could not be totally ruled out but was assumed to be very small as indicated by the only minor increase in the light scatter peak. The copper concentration was varied between 10^{-5} and 10^{-7} M without a detectable influence on the observed NOM fluorescence decay.

The first results of experiments with alumina and iron indicated that both metal ions influenced the NOM fluorescence decay. In the presence of iron(II) at pH 3 the fluorescence decay time distribution was shifted toward shorter decay times. The ratio of the three mean fluorescence decay times found in the distribution analysis without and with iron(II) present was the same (τ_x / $\tau_x^{HS} \sim 1.2$, $x = 1,2,3$). The dynamic quenching of the

iron(II) was dependent on the emission wavelength and was increased at shorter emission wavelengths. The fact that iron(II) equally influenced all fluorescence decay times made an interpretation in terms of a nonspecific dynamic interaction process tempting.

Al^{3+} also effected the fluorescence decay of the bog lake water FA investigated. However, the observed dynamic quenching was smaller compared to iron(II), the three mean fluorescence decay times were altered to an different extent, and moreover, the obtained pattern in the decay time distribution seemed to change upon the complexation of Al^{3+}.

In further experiments the lanthanide ions europium and terbium were introduced. Here, the influence on the NOM fluorescence decay was monitored as well as the luminescence of the lanthanide ions themselves, indicating energy transfer from the NOM ligands to the lanthanide ions. In the time-resolved fluorescence measurements it was found that the observed change in the NOM fluorescence decay was dependent on the detection wavelength. For fluorescence emission wavelengths greater than 400 nm a quenching of the NOM fluorescence decay was found, whereas for shorter wavelengths the opposite effect was monitored. These results are describe in more detail in a separate paper [36]. Investigations of the interaction between metal ions and NOM are a subject of current research projects.

CONCLUSIONS

The application of global analysis with three exponential decay terms and the distribution analysis revealed similar tendencies for the fluorescence decay times and the related fractional intensities. Within the experimental uncertainty identical fluorescence decay times could indicate that similar fluorescence structures are present in the investigated NOM samples. Based on the results reported for the fluorescence decay of NOM, it is tempting to attribute a key position to the presence of heteroatoms. However, this conclusion has been based on a small number of NOM samples, and further investigations are needed. It is well proven that a great part of the nitrogen content of NOM can be attributed to bound amino acids [33]. Work is in progress to investigate the influence of enzymatic hydrolysis of the bound amino acids on the fluorescence of the municipal wastewater effluent and on the observed emission wavelength dependence of fractional intensities A_x.

Another parameter that should be related to the observed fluorescence of the investigated NOM sample is the metal ion content, especially that of paramagnetic metal ions. Paramagnetic metal ions show the strongest fluorescence intensity quenching. In our experiments with metal ions different effects on the fluorescence decay were indicated. Measurements to determine the content of metal ions in the used NOM samples are in progress. Preliminary results show that, especially, the iron content is considerablely high for all NOM samples investigated (several hundred micrograms per gram of DOC) [34]. The important role of the iron(III)/iron(II) balance in photochemical reactions in the presence of NOM in surface waters is well known [35], but its role for NOM fluorescence has to be elucidated. The application of lanthanide ions, especially europium and terbium, is promising because the metal ion luminescence offers an additional detection parameter. The fact that some of the energy level in the europium complexes is located below 400 nm might explain the observed wavelength dependence on the fluorescence decay. Experiments with other lanthanide ions with different energy levels are planed in order to investigate this influence to a deeper extent.

Based on these results of fractionation using size exclusion chromatography, it is tempting to assume a quite homogeneous distribution of fluorescence subunits inside the investigated FA, probably produced in the XAD isolation procedure or caused by the similarities in the educts from which the NOM samples were descended.

The suggested connection between nominal molar mass and observed fluorescence is supported by the investigations of the influence of the ozone on the NOM fluorescence decay. Experiments with NOM samples fractionated based on, e.g., hydrophobicity will further elucidate the effect of the molar mass on NOM fluorescence decay.

ACKNOWLEDGMENTS

The authors wish to thank the Deutsche Forschungsgemeinschaft (DFG) for funding great parts of the work in the ROSIG program. Further, they are grateful to A. Heidt for the isolation and fractionation of the fulvic acid fractions and to A. Wolf for ozonation of the NOM sample. They also wish to thank R. Klenze for supplying the Eu^{3+} solutions.

REFERENCES

1. P. J. Shaw, R. I. Jones, and H. DeHaan (1994) *Environ. Technol.* **15**, 765–774.

2. D. B. Wagoner, R. F. Christman, G. Couchon, and R. Paulson (1997) *Environ. Sci. Technol.* **31**, 937–941.
3. G. Abbt-Braun, U. Schmiedel, and F. H. Frimmel (1990) *Vom Wasser* **75**, 59–73.
4. H.-R. Schulten, G. Abbt-Braun, and F. H. Frimmel (1987) *Environ. Sci. Technol.* **21**, 349–357.
5. G. Abbt-Braun, F. H. Frimmel, and H.-R. Schulten (1990) *Vom Wasser* **74**, 325–338.
6. J. A. Leenheer, R. L. Wershaw, and M. M. Reddy (1995) *Environ. Sci. Technol.* **29**, 399–405.
7. W. Liao, R. F. Christman, J. D. Johnson, D. S. Millington, and J. R. Hass (1982) *Environ. Sci. Technol.* **16**, 403–409.
8. S. Huber, T. Gremm, and F. H. Frimmel (1990) *Vom Wasser* **75**, 331–342.
9. T. M. Miano, G. Sposito, and J. P. Martin (1988) *Soil Sci. Soc. Am. J.* **52**, 1016–1019.
10. J. J. Mobed, S. L. Hemmingsen, J. L. Autry, and L. B. McGown (1996) *Environ. Sci. Technol.* **30**, 3061–3065.
11. G. Abbt-Braun and F. H. Frimmel (1991) *Vom Wasser* **77**, 291–302.
12. R. R. Engebretson and R. von Wandruszka (1994) *Environ. Sci. Technol.* **28**, 1934–1941.
13. S. E. Cabaniss (1992) *Environ. Sci. Technol.* **26**, 1133–1139.
14. M. J. Pullin and S. E. Cabaniss (1995) *Environ. Sci. Technol.* **29**, 1460–1467.
15. S. Chen, W. P. Inskeep, S. A. Williams, and P. R. Callis (1994) *Environ. Sci. Technol.* **28**, 1582–1588.
16. M. U. Kumke, H.-G. Löhmannsröben, and Th. Roch (1994) *Analyst* **119**, 997–1001.
17. C. H. Lochmüller and S. S. Saavedra (1986) *Anal. Chem.* **58**, 1978–1981.
18. J. F. Power, R. LeSage, D. K. Sharma, and C. H. Langford (1986) *Environ. Technol. Lett.* **7**, 425–430.
19. L. B. McGown, S. L. Hemmingsen, J. M. Shaver, and L. Geng (1995) *Appl. Spectrosc.* **49**, 60–66.
20. R. L. Cook and C. H. Langford (1995) *Anal. Chem.* **67**, 174–180.
21. M. U. Kumke, G. Abbt-Braun, and F. H. Frimmel (1998) *Acta Hydrochim. Hydrobiol.* **26**, 73–81.
22. P. J. Milne and R. G. Zika (1989) *Marine Chem.* **27**, 147–164.
23. U. Zimmermann, H.-G. Löhmannsröben, and T. Skrivanek (1997). *Proceedings EUROPTO Series: Remote Sensing of Vegetation and Water, and Standardization of Remote Sensing Methods* Vol. 3107, pp. 239–249.
24. G. Abbt-Braun, F. H. Frimmel, and P. Lipp (1991) *Z. Wasser-Abwasser-Forsch.* **24**, 285–292.
25. A. Wolf and F. H. Frimmel (1997) *Proceedings of the 7th International Symposium: Chemical Oxidation Technology for the Nineties*, Nashville, TN (in press).
26. D. M. Gamsky, A. A. Goldin, E. P. Petrov, and A. N. Rubinov (1992) *Biophys. Chem.* **44**, 47–60.
27. D. R. James and W. R. Ware (1986) *Chem. Phys. Lett.* **126**, 7–11.
28. A. Siemiarczuk, B. D. Wagner, and W. R. Ware (1990) *J. Phys. Chem.* **94**, 1661–1666.
29. J.-C. Brochon, A. K. Livesey, J. Pouget, and B. Valeur (1990) *Chem. Phys. Lett.* **174**, 517–522.
30. C. F. Scheck, F. H. Frimmel, and A. M. Braun (1992) *Z. Naturforsch.* **47b**, 399–405.
31. F. H. Frimmel and W. Hopp (1986) *Fresenius Z. Anal. Chem.* **325**, 68–72.
32. G. Bidogilio, I. Grenthe, P. Qi, P. Robouch, and N. Omenetto (1991) *Talanta* **9**, 999–1008.
33. J. B. Jahnel and F. H. Frimmel (1995) *Acta Hydrochim. Hydrobiol.* **23**, 31–35.
34. G. Abbt-Braun (1997) Personal communication.
35. B. C. Faust and R. G. Zepp (1993) *Environ. Sci. Technol.* **27**, 2517–2522.
36. C. Tiseanu, M. U. Kumke, F. H. Frimmel, R. Klenze, and J. I. Kim (1998) *J. Photochem. Photobiol. A* (in press).